https://doi.org/10.5194/egusphere-2026-986
Preprint. Discussion started: 16 June 2026

Performance and Controlling Factors of Airborne LiDAR Snow Depth Estimates in Boreal Forests: Insights from NASA SnowEx 2023 Alaska Campaign

Jipeng Liu[1], Eunsang Cho[1], Carrie Vuyovich[2]

[1]Ingram School of Engineering, Texas State University, San Marcos, TX, USA
[2]Hydrological Sciences Laboratory, NASA Goddard Space Flight Center, Greenbelt, MD, USA

Correspondence to: Eunsang Cho (eunsang.cho@txstate.edu)

Abstract. Quantifying spatial distribution of the snowpack is crucial for hydrological, ecological, and climate research, as well as their applications. Due to the high spatial resolution and extensive coverage, Airborne Light Detection and Ranging (LiDAR) has emerged as an effective tool for large-scale snow depth estimation. However, discrepancies between LiDAR-derived and manually measured snow depth values exist across areas influenced by topographical and vegetation characteristics such as canopy height, slope, and roughness. This study aims to 1) evaluate the performance of the airborne LiDAR snow depth measurements compared to magnaprobe in-situ data and 2) identify key factors affecting the accuracy of airborne LiDAR snow depth measurements focusing on the boreal forest environment. We utilize airborne LiDAR data and ground-based snow depth observations collected in the Fairbanks region of central Alaska during NASA SnowEx 2023 Alaska Campaign. The study focuses on three subregions: Bonanza Creek Experimental Forest (BCEF), Farmers Loop Creamers Field (FLCF), and Caribou-Poker Creeks Research Watershed (CPCRW). The results showed that the LiDAR snow depth data has a reasonable agreement with in-situ observations (R: 0.605, Mean Absolute Error: 18.8 cm) but exhibits varying levels of errors across the three subregions. By applying regression analysis and machine learning, we quantify the contribution of individual factors to measurement discrepancies and determine which factors are most influential. We employed Gradient Boosting Machine (GBM) model using five LiDAR-derived environmental variables—canopy height, elevation, slope, roughness, and ground point density—as predictors of relative error. Across all subregions and models, canopy height consistently emerged as the most important factor of LiDAR snow depth error.

Keywords: Snow depth, Airborne LiDAR, Remote sensing, NASA SnowEx

https://doi.org/10.5194/egusphere-2026-986
Preprint. Discussion started: 16 June 2026

1. Introduction

Snow plays a critical role in global hydrological and ecological processes. It provides a crucial source of water for streamflow and reservoirs and controls the land-atmosphere energy fluxes (Li et al., 2017; Siirila-Woodburn et al., 2021; Sturm et al., 2017). Seasonal snowpack acts as a natural aquifer, releasing water during the snowmelt season and influencing global climate by its high albedo and insulating effect on the ground (Xu & Dirmeyer, 2013; Blau et al., 2024). In snow-dominant watersheds, a substantial portion of annual streamflow comes from snowmelt – up to 75% in some Western North American basins – underscoring the importance of accurately measuring snow volume (Stewart et al., 2004; Fritze et al., 2011). Beyond total snow water storage, the spatial distribution of snow depth is also critical; heterogeneous snow cover (patchy or nonuniform snowpacks) strongly controls melt patterns, soil freeze/thaw dynamics, and ecological processes at the landscape scale (Lundquist & Dettinger, 2005). For instance, variations in terrain and vegetation can lead to preferential snow accumulation in certain areas and early melt in others, affecting streamflow timing and habitat conditions (Varhola et al., 2010; Guan et al., 2023).

However, measuring snow depth distribution across large and remote areas is challenging. In situ methods (e.g., snow probes and snow courses) provide accurate point measurements but are labor-intensive and cover limited spatial extents (Sturm et al., 2015). Remote sensing enables mapping snow depth across broad areas, but traditional satellite-based techniques (such as passive microwave) have had limited success in measuring snow depth at fine spatial scales, especially under forest canopies (Stillinger et al., 2023; Luo et al., 2022; Rittger et al., 2020; Demil et al., 2025). Forested environments pose particular difficulties: tree canopies intercept a significant portion of snowfall (30–80% in dense conifer forests) before it reaches the ground, and they obscure the snow from many sensors (Lumbrazo et al., 2022). Consequently, snow depths in forests tend to be shallower and more spatially variable compared to open areas (Dharmadasa et al., 2024). Ground-based and even spaceborne sensors often cannot “see” the snow under trees, leading to data gaps or biases in forested regions (Demil et al., 2025).

Airborne LiDAR (Light Detection and Ranging) has emerged as a promising solution for high-resolution snow depth mapping in complex terrains, including forests. LiDAR actively emits laser pulses and measures their returns, capable of penetrating gaps in canopy to reach the snow surface or ground (Painter et al., 2016; Mazzotti et al., 2019; Deschamps-Berger et al., 2020; Currier et al., 2019, Deems et al., 2013). Modern airborne LiDAR systems can achieve vertical accuracies on the order of decimeters and point densities of order 1 point/m² or greater, making it possible to detect snow depth by comparing snow-on and snow-off surface elevations. Notably, LiDAR in near-infrared wavelengths can even map sub-canopy topography to some extent, which is a major advantage over passive optical methods (Clark & Clark, 2004). Over the past decade, numerous studies have demonstrated LiDAR’s utility for snow depth estimation. For example, Deems et al (2013) provided an extensive review of LiDAR snow measurement, noting typical airborne LiDAR vertical uncertainties of ~0.10–0.25 m in open areas and the ability to capture snow depth spatial variability that is unattainable with traditional methods. In addition to traditional airborne platforms, recent advances have

https://doi.org/10.5194/egusphere-2026-986
Preprint. Discussion started: 16 June 2026

enabled the use of Unpiloted Aerial Systems (UAS), or drone-based LiDAR, for snow depth mapping. These systems offer finer spatial resolution and greater flexibility for surveying small or difficult-to-access regions, making them increasingly popular for snow research in forested environments. More recent work with UAS LiDAR in New Hampshire showed that high-density LiDAR point clouds could measure a shallow 10 cm snowpack with ~1 cm error in open fields, though errors increased to ~10 cm under forest canopy (Jacobs et al., 2021). This highlights that while LiDAR substantially improves snow mapping, its accuracy can degrade in the presence of dense vegetation, where fewer laser pulses reach the ground and the snow surface itself may be harder to discern (Dharmadasa et al., 2022).

The influence of vegetation on LiDAR snow depth accuracy is a key concern in boreal forest environments (May et al., 2025). Tall canopy and complex understory can cause LiDAR to underestimate snow depth because some fraction of laser pulses are intercepted by branches or attenuated, resulting in fewer ground returns. The presence of snow on tree branches can also confuse the classification of returns (e.g., a LiDAR return from snow-covered downed logs might be mistakenly taken as the ground). Terrain characteristics further complicate measurements: on steep slopes, horizontal displacement of returns and pulse footprint enlargement can introduce elevation errors, and rough terrain or boulders can create uncertainty when differentiating snow surface changes (Jacobs et al., 2021). Indeed, prior studies have suggested a range of physical factors that affect snow depth distribution and measurement. For instance, variability in snow depth has been linked to topographic features (elevation, slope, aspect, terrain roughness) and vegetation structure (Hojatimalekshah et al., 2021; 2023, Meriö et al., 2023). In relatively open environments, elevation and wind redistribution lead to deeper snow at higher elevations or in lee aspects, whereas forests reduce snow accumulation via canopy interception and sublimation losses (Gustafson et al., 2010; Dadic et al., 2010). These same factors likely influence the agreement between LiDAR and ground measurements: where snow is very shallow (e.g., under dense canopy or on windswept ridges), even small absolute errors can be a large relative fraction, and where terrain is steep or highly irregular, co-registration errors can occur.

Despite the recognized potential of airborne LiDAR, there is a need for systematic assessment of its accuracy in forested regions and an understanding of what conditions lead to larger errors. While airborne LiDAR has been widely tested in alpine or temperate forest environments, relatively few studies have focused on boreal forests, which are characterized by cold climates, discontinuous permafrost, and dense conifer canopies. These unique features strongly influence both snow accumulation and LiDAR performance, making boreal forests a distinct and understudied environment in snow remote sensing (NASA, 2018). The NASA SnowEx 2023 campaign in Alaska provides an ideal opportunity to evaluate LiDAR snow depth retrievals in a boreal forest setting across varying conditions. By combining airborne LiDAR data with an extensive set of ground truth measurements and environmental variables, we can quantify how well LiDAR performs and what drives any discrepancies.

In this study, we address the following questions: (1) How well do airborne LiDAR-derived snow depths correspond to in-situ snow depth observations across boreal forest sites? (2) What are the main environmental

https://doi.org/10.5194/egusphere-2026-986
Preprint. Discussion started: 16 June 2026

factors that affect the magnitude of LiDAR snow depth measurement error in these forested environments? (3) Are these factors consistent across different forest sites, or do certain locations exhibit unique influences? To answer these, we evaluate LiDAR snow depth accuracy at three sites in interior Alaska, and we use statistical and machine learning approaches to determine the contribution of canopy, terrain, and LiDAR sampling characteristics to the observed errors. By identifying the dominant drivers of error, our goal is to improve the use of LiDAR for snow monitoring in forests. This work will help inform best practices for future LiDAR-based snow surveys and guide interpretation of SnowEx data for hydrological modeling and remote sensing product development.

2. Study Area

The study was conducted in the boreal forest region of interior Alaska, near Fairbanks, as part of the NASA SnowEx 2023 Alaska campaign. Three primary subregions were selected for intensive observations (Figure 1): (1) Bonanza Creek Experimental Forest (BCEF), (2) Farmers Loop/Creamer's Field (FLCF), and (3) Caribou-Poker Creek Research Watershed (CPCRW). These sites are all within the discontinuous permafrost zone of central Alaska and encompass a range of forest and terrain conditions typical of the boreal ecosystem.

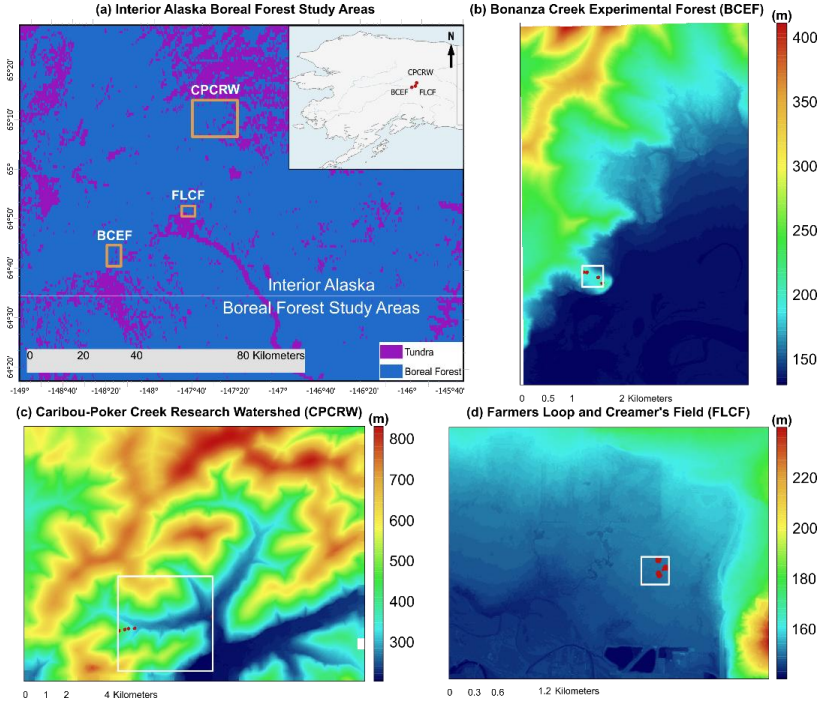

Figure 1. Map of the Fairbanks, Alaska study areas. The panels show the three study sites: (a) Interior Alaska Boreal Forest Study Areas, (b) Bonanza Creek Experimental Forest (BCEF), (c) Caribou-Poker Creek Research Watershed (CPCRW), and (d) Farmers Loop and Creamer's Field (FLCF). The white boxes in each panel indicate the zoomed-in regions shown in Figure 2 for detailed analysis of environmental variables

https://doi.org/10.5194/egusphere-2026-986
Preprint. Discussion started: 16 June 2026

BCEF is located ~20 km southwest of Fairbanks and includes both lowland floodplain forests and upland rolling hills within the Tanana River valley. Vegetation at BCEF is dominated by mature spruce and birch forest in the uplands and mixed hardwood-conifer stands in lowlands; the area includes some experimental plots managed by the Bonanza Creek Long Term Ecological Research program. The terrain at BCEF is gently to moderately sloping (elevations ~130–300 m ASL) with patches of permafrost and seasonal wetlands. CPCRW is a 104 km² research watershed northeast of Fairbanks in the Caribou-Poker Creeks area, featuring more complex topography and higher elevation forests. Elevations in CPCRW range from ~200 m in valley bottoms to over 700 m on ridges. The vegetation is typical interior Alaska boreal forest: black and white spruce, as well as deciduous aspen and birch in warmer aspects, with tree density varying from dense valley forests to more sparse stands near treeline. CPCRW contains steep slopes, incised valleys, and a mosaic of permafrost conditions, making it a challenging but representative site for studying snow in forested terrain. FLCF refers to adjacent wildlife refuge area and research site within Fairbanks (Creamer's Field and Farmers Loop, respectively), characterized by a mix of open fields, secondary-growth boreal forest, and wetlands. The FLCF area is relatively flat (130–180 m ASL) and includes open meadow/pasture areas (e.g., Creamer's Field waterfowl refuge) adjacent to birch-spruce woodlands; it represents a more open forest environment within the discontinuous permafrost zone. The regional climate of interior Alaska is subarctic continental, with cold, relatively dry winters. Fairbanks experiences mean January temperatures around –20 °C and an average winter (October–April) snowfall on the order of 150–200 cm, although snow depth on the ground by late winter is typically 50–80 cm due to mid-winter sublimation and settling. The winter of 2022–2023 (during SnowEx) featured typical conditions with sustained snow cover from October through April. In forested areas, snow depths tend to be lower under canopy than in open areas due to interception; field observations in the region have shown significant differences in snow depth between forested and open areas in Interior Alaska (May et al., 2025), although the specific range of snow depth variability may vary regionally and interannually. This range of conditions across the three study sites provides a robust testbed for airborne LiDAR snow depth estimation: BCEF and CPCRW include dense canopy and sloping terrain, whereas parts of FLCF offer open, flat reference areas.

3. Datasets and Methods

3.1 Airborne LiDAR

Airborne LiDAR surveys were conducted as part of SnowEx 2023 to capture the terrain and snow surface at each site. The LiDAR system was flown on a fixed-wing aircraft (a Cessna T206) equipped with a Riegl VQ-580ii airborne laser scanner. This sensor operates at a near-infrared wavelength of 1064 nm and is capable of detecting multiple returns per pulse. Key sensor specifications include a scanning field of view of ±37.5° off-nadir (75° total sweep) and an inertial navigation system (INS) Applanix POS AV system for precise positioning and orientation. The LiDAR system was flown at approximately 700 m above ground level, at an airspeed of ~200 km/h (110 knots) over the study areas. Flight lines were planned to ensure high overlap

https://doi.org/10.5194/egusphere-2026-986
Preprint. Discussion started: 16 June 2026

(>50% side lap between adjacent swaths) and to cover each site completely. At 700 m AGL with 75° FOV, each flight swath covered roughly ~1 km width on the ground. Adjacent flight lines were spaced to provide overlapping coverage, effectively increasing total point density and reducing the likelihood of data gaps beneath tree canopies (Vuyovich et al., 2022). Two LiDAR acquisitions were used: a snow-off flight conducted in May 2022 (bare ground baseline) and a snow-on flight on 11 March 2023 (late winter, peak snowpack). Both flights covered all three study areas (BCEF, FLCF, and CPCRW) under clear conditions. The May snow-off LiDAR captured the bare-earth topography and vegetation structure, while the March flight captured the snow-covered surface. The LiDAR data were processed to produce point clouds and gridded digital elevation models (DEMs) (Larsen 2024a). The point cloud density for a single pass was on the order of ~10 points/m² on average. Thanks to overlapping flight lines, the effective point density at most locations exceeded 20 points/m². This high density improves the chances of penetrating to the ground in forested areas by providing multiple viewing angles. The raw point clouds were classified into ground and non-ground returns using standard LiDAR processing algorithms (e.g., iterative filtering) to separate the terrain surface from vegetation and other returns.

From the classified point clouds, terrain models and snow surface models were derived (Larsen 2024b). The snow-off (May) ground returns were interpolated to create a high-resolution digital terrain model (DTM) representing the bare earth elevation (and also canopy height models by difference from first returns). The snow-on (March) point cloud was processed to obtain the elevations of the snow surface. In open areas, snow-on ground returns directly reflect the snow surface. Under canopy, fewer ground returns are typically recorded; in these areas, any last-return points that likely correspond to the snow surface or ground were used, supplemented by interpolation from surrounding returns. The end product for each site was a snow depth raster at 0.5 m resolution (chosen to balance detail and noise) calculated as the difference between the snow-on surface and the snow-off ground surface at each grid cell. This LiDAR-derived snow depth map is essentially a spatial differencing of the two LiDAR DEMs. Areas with no valid returns in March (e.g., extremely dense canopy with no ground or snow returns) were masked out or filled using nearest-neighbor extrapolation from adjacent areas where data existed. (NASA, 2025)

3.2 Ground-based Snow Depth Measurements

Extensive in-situ snow depth measurements were collected to validate and evaluate snow remote sensing datasets. NASA SnowEx23 field teams visited each study area around the time of the late winter LiDAR flight (early to mid March 2023) and measured snow depth using manual probes. Within each site, multiple plots and transects were established to capture local variability. Measurement locations were recorded with manual probe GPS units. In total, 13 individual study plots, N = 1,045 snow depth measurements, were used in this analysis (this is the combined number of points across the 13 study plots at all three sites on March 11, 2023). Care was taken to sample a range of conditions: beneath different canopy densities (open vs under tree canopy), different slope positions (ridge, mid-slope, valley), and varying aspects. At each location, depth was

https://doi.org/10.5194/egusphere-2026-986
Preprint. Discussion started: 16 June 2026

measured by pushing a snow probe to the ground (or top of vegetation if vegetation protruded through snow, in which case those points were noted). The measurement uncertainty for manual probe readings on level ground is on the order of ±12 cm (Stuefer et al., 2025). Under uneven forest-floor conditions, additional uncertainty of a few centimeters may occur when the exact ground surface is difficult to identify. These in-situ measurements serve as ground truth to compare against LiDAR-derived snow depths extracted at the corresponding locations. To compare with LiDAR, the coordinates of each ground measurement were used to sample the LiDAR snow depth map. Each ground measurement thus has a corresponding LiDAR-estimated depth value. We then calculated error statistics per point:

$$Relative\ error = (LiDAR\ snow\ depth - in\_situ\ snow\ depth) / in\_situ\ snow\ depth \quad \textit{eq. (1)}$$

at each location. A positive error indicates LiDAR overestimated depth, and negative indicates underestimation.

3.3 Physical Variables

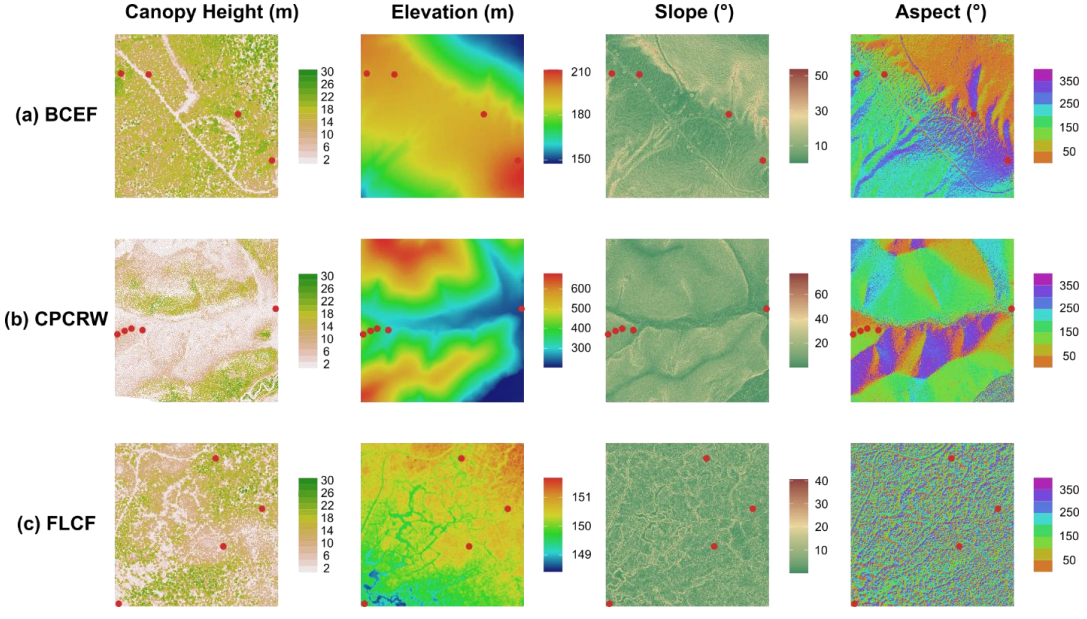

Figure 2. Canopy Height, Elevation, Slope, and Aspect over study regions. Environmental variables were derived from NASA SnowEx23 airborne LiDAR datasets and associated products. Canopy height was calculated by differencing the DSM and DTM. Elevation, slope, and aspect were extracted from the SnowEx-derived DTM. The maps correspond to the study regions BCEF, FLCF, and CPCRW, all located near Fairbanks, Alaska. Red dots indicate the locations of manual snow depth measurement sub-regions within each study site.

In order to investigate factors influencing the LiDAR errors, we derived a set of environmental predictor variables at each measurement location. Five variables were considered, all obtained or derived from the LiDAR datasets and associated products:

https://doi.org/10.5194/egusphere-2026-986
Preprint. Discussion started: 16 June 2026

3.3.1 Canopy Height

The height of the vegetation canopy above the ground (Larsen 2024b). This was derived from the snow-off LiDAR by computing the difference between first-return DSM (digital surface model) and the DTM. Canopy height is a proxy for vegetation density and structure – taller (and typically denser) canopy was expected to reduce LiDAR penetration and hence potentially increase snow depth misestimation.

3.3.2 Elevation

The ground elevation (Larsen 2024a) at the point. This captures large-scale topographic position. Elevation can correlate with snow climate (higher elevations might have more snow accumulation) and with certain errors if there were any biases in LiDAR or GPS with altitude, although here it mainly serves to distinguish the sites and internal variability (CPCRW spans a larger elevation range than FLCF, for example).

3.3.3 Slope

The local terrain slope (in degrees), derived from the digital terrain model (DTM) using a 3×3 pixel moving window (~1.5 m × 1.5 m). Steeper slopes may introduce greater LiDAR elevation error due to the geometry of pulse returns and also often have thinner snow cover due to preferential snow shedding and wind effects. We hypothesized that LiDAR snow depth error magnitude might increase on steeper slopes.

$$Slope = \arctan\left(\sqrt{\left(\frac{\partial z}{\partial x}\right)^2 + \left(\frac{\partial z}{\partial y}\right)^2}\right) \quad \text{eq. (2)}$$

3.3.4 Roughness

A measure of micro-topography or surface irregularity. We quantified roughness as the standard deviation of elevation within a 3×3 pixel moving window (~1.5 m × 1.5 m area) around each point (using the DTM). Higher values indicate very uneven ground (e.g., boulders, shrubs, hummocks) whereas low values indicate smooth ground. Rough terrain could affect snow depth retrieval because if the ground is uneven, small misalignments in snow-on vs snow-off surfaces can produce spurious snow depth differences. Also, roughness can correspond to certain vegetation undergrowth or ground cover that might influence snow accumulation.

$$Roughness = \sqrt{\frac{1}{n-1}\sum_{i=1}^{n}(z_i - \bar{z})^2} \quad \text{eq. (3)}$$

3.3.5 Ground Point Density

The density of LiDAR ground returns in the snow-on dataset at each location (points per square meter). This was calculated by counting the number of points classified as ground in the snow-on LiDAR within a 0.5 m radius of the point, and dividing by area to get density. This variable directly indicates the amount of LiDAR penetration through canopy: a low ground return density under a thick canopy means the LiDAR had difficulty reaching the ground. We expect that lower point density (i.e., sparse returns) could be associated with larger errors, as the interpolation of snow surface might be less certain in those areas. In contrast, areas with very high ground return density (e.g., open fields) likely have very accurate LiDAR snow depth measurements.

https://doi.org/10.5194/egusphere-2026-986
Preprint. Discussion started: 16 June 2026

3.4 Accuracy Assessment

We first assessed the overall accuracy of the LiDAR snow depth estimates by comparing them directly with the in-situ measurements. We computed summary statistics including the mean error (bias), mean absolute difference (MAD), root mean square error (RMSE), and the Pearson correlation coefficient (R) between LiDAR-derived and measured depths. These metrics were computed for the pooled dataset of all sites combined, as well as separately for each of the three study sites to see if accuracy differed by location. A one-to-one scatter plot of LiDAR vs. in-situ depth was used to visualize the agreement and any systematic bias. We also tested the correlation between error magnitude and each predictor variable individually (e.g., using Pearson correlation) as an initial check.

3.5 Variable Importance

To address the second objective (identifying key factors driving LiDAR error), we employed a machine learning regression model to predict the LiDAR snow depth error at each point from the environmental variables. Gradient Boosting Machine (GBM), a widely used ensemble learning method, was chosen for its strong performance in capturing nonlinear relationships and variable interactions (Friedman, 2001; Elith et al., 2008). GBM have been successfully applied in various environmental and remote sensing contexts, including snow depth and vegetation modeling (Lary et al., 2016; Zhao et al., 2021). GBM also provides variable importance rankings and allows for interpretability via partial dependence plots, which are commonly used in remote sensing applications to visualize the marginal effect of each predictor (Zhao et al., 2021). Prior studies have demonstrated that GBM often outperform simpler linear models and even SVM in geospatial prediction tasks, especially where variable interactions are strong and heterogeneous (Pelletier et al., 2019).

The response variable for modeling was the relative error in snow depth, defined as (LiDAR depth – in-situ depth) / in-situ depth. We chose relative error (dimensionless, expressed as a fraction) to normalize for the fact that deeper snow measurements could tolerate a larger absolute error. This also helps stabilize variance if, for example, one site had generally deeper snow than another. Points with very shallow snow (< 10 cm) were treated carefully in relative error computation to avoid blowing up the fraction (in such cases, we also considered absolute error models for comparison). We trained separate models for each site. Training on each site's data (roughly 300 points per site) allows us to see if the importance of factors changes with location. Hyperparameters for GBM (like number of trees, learning rate, max depth) were tuned via grid search.

The performance of each model was evaluated by the coefficient of determination (R^2) on predicted vs observed errors and by RMSE of the error prediction. Importantly, the GBM model provides a ranking of predictor importance (often based on the number of splits or gain improvement provided by each variable). We recorded the relative importance of the five variables for each model. In addition, partial dependence plots were generated for the GBM to visualize how each predictor affects the predicted error when controlling for others. For the best-performing model in each site, we used it to predict snow depth error across the landscape at that site, producing a spatial map of predicted LiDAR error. This was done by feeding the gridded layers of

https://doi.org/10.5194/egusphere-2026-986
Preprint. Discussion started: 16 June 2026

canopy height, slope, etc., at that site into the trained model. The result is a raster of expected error (as a percentage or fraction) for each pixel, which we compare qualitatively to observed error patterns.

4. Results

4.1 Accuracy Evaluation

The airborne LiDAR surveys successfully mapped snow depth across all three areas, but with some differences in accuracy when validated against in-situ manual probe observations. Overall, considering all available paired observations (1,045 points) pooled from the three study sites, the LiDAR-derived snow depths showed a moderate correlation with in-situ measurements (Pearson R = 0.60). This pooled correlation was slightly higher than the strongest site-specific correlation observed in FLCF (R = 0.55), likely reflecting the larger sample size and broader range of environmental conditions represented in the combined dataset. The MAD and RMSE were 0.17 m and 0.22 m, respectively, indicating that LiDAR generally underestimated snow depth. These underestimations were consistent across three areas (Figure 3).

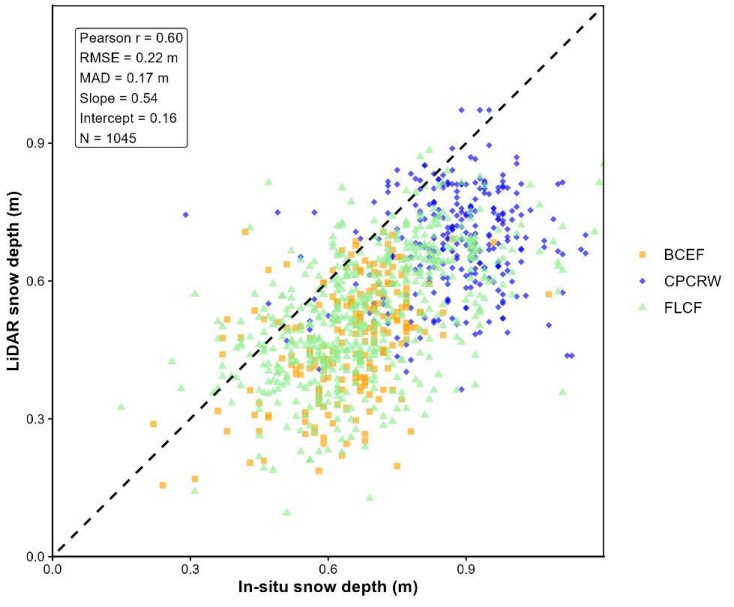

Figure 3. Comparison of LiDAR-derived snow depth vs. in-situ measured snow depth for all validation points (all sites combined). The dashed line is the one-to-one line. A moderate correlation (R ≈ 0.60) is observed, and the mean absolute difference is on the order of 0.17 m. Points falling below the one-to-one line indicate LiDAR underestimation (common under dense canopy), whereas points above indicate LiDAR overestimation.

When examining the sites individually, some differences emerge. Among the three sites, FLCF exhibited the strongest agreement between LiDAR and ground measurements. The correlation at FLCF was around 0.55, MAD was 0.18 m and RMSE was 0.21m. Points at FLCF were almost all located in areas characterized by a mixture of open and wooded cover over flat to gently rolling terrain where LiDAR performed very well, raising the site's overall accuracy. Under

https://doi.org/10.5194/egusphere-2026-986
Preprint. Discussion started: 16 June 2026

forested areas identified by higher canopy heights in Figure 4b, errors were generally larger than those observed in adjacent open areas. (Figure 4).

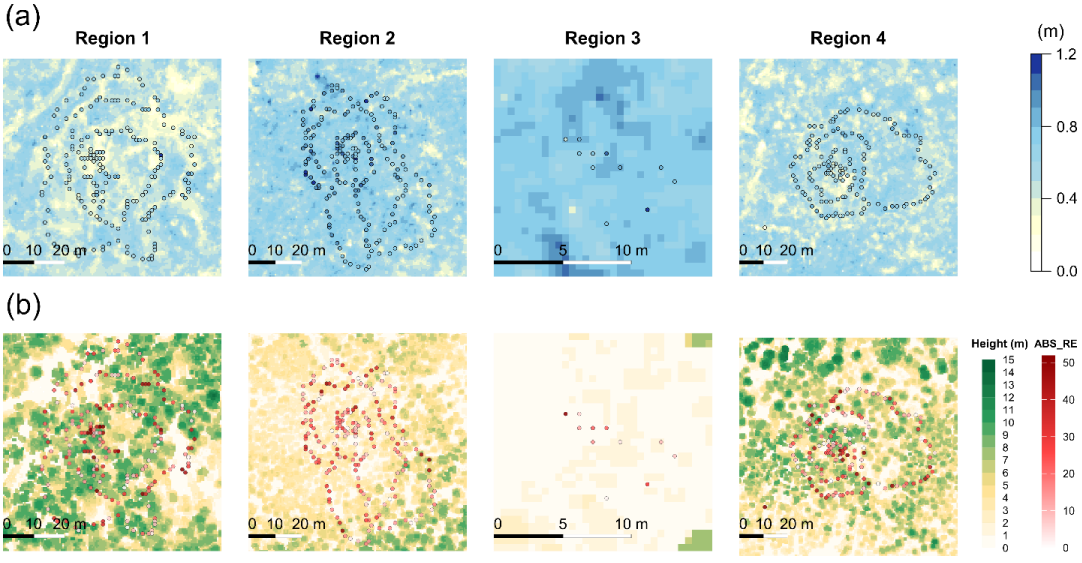

Figure 4. LiDAR Snow Depth, Canopy Height, and Error Distribution in the FLCF Study Area. (a) LiDAR-derived snow depth map for the Farmers Loop and Creamer's Field (FLCF) region, overlaid with in-situ manual snow depth measurements (color circles). The background raster displays snow depth estimated using airborne Light Detection and Ranging (LiDAR), while the black circles represent manual field measurements. The four marked sub-regions (1–4) highlight clustered areas for localized comparison. (b) Spatial Distribution of Absolute Relative LiDAR Snow Depth Errors and Canopy Height at FLCF.

In BCEF, LiDAR tended to underestimate snow depth under mature spruce stands. The correlation was lower (R = 0.44), and MAD was 0.19 m. We observed that in some forest plot locations at BCEF, ground-based snow depths around 50 cm corresponded to LiDAR estimates of only ~30 cm, a substantial underestimation. In more open parts of BCEF, LiDAR was accurate. This variability lowered the overall correlation. The bias at BCEF was about –18 cm (LiDAR underestimating on average) (Figure 5).

CPCRW had the lowest raw correlation (R =0.16) and the largest errors in absolute terms (MAD =0.21 m). This site had the most challenging conditions: steep slopes and dense spruce forest in many areas. Notably, a number of CPCRW points on slopes under dense canopy showed LiDAR snow depths less than half of the actual measured depth (e.g., LiDAR ~57 cm vs actual ~110 cm). The bias at CPCRW was around –19 cm (underestimate). Despite these errors, LiDAR still captured general patterns: Errors tended to be larger in areas characterized by dense canopy and complex terrain. (Figure 6). Error distribution across these sites clearly indicates that LiDAR performance is optimal in open or lightly vegetated terrain and poorest in densely forested and rugged areas. Open and sparsely vegetated areas consistently showed lower errors. Conversely, dense forests, particularly at CPCRW, demonstrated significantly larger errors, often exceeding 20 cm due to limited penetration of LiDAR signals to the snow surface under dense canopy

https://doi.org/10.5194/egusphere-2026-986
Preprint. Discussion started: 16 June 2026

conditions.

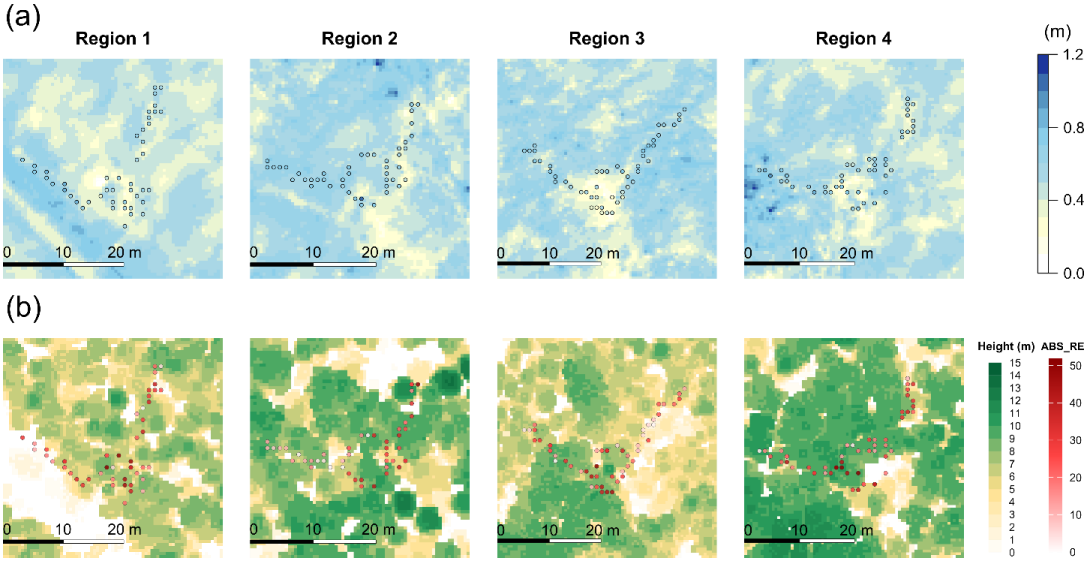

Figure 5. LiDAR Snow Depth, Canopy Height, and Error Distribution in the BCEF Study Area. (a) LiDAR-derived snow depth map for the Bonanza Creek Experimental Forest (BCEF) region, overlaid with in-situ manual snow depth measurements (color circles). The background raster displays snow depth estimated using airborne Light Detection and Ranging (LiDAR), while the black circles represent manual field measurements. The four marked sub-regions (1–4) highlight clustered areas for localized comparison. (b) Spatial Distribution of Absolute Relative LiDAR Snow Depth Errors and Canopy Height at BCEF.

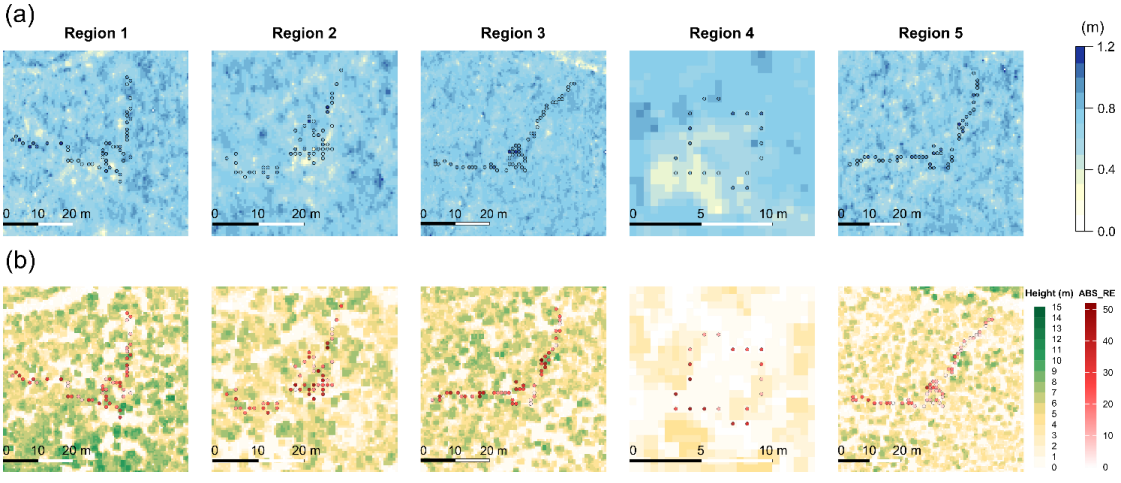

Figure 6. LiDAR Snow Depth, Canopy Height, and Error Distribution in the CPCRW Study Area. (a) LiDAR-derived snow depth map for the Caribou-Poker Creek Research Watershed (CPCRW) region, overlaid with in-situ manual snow depth measurements (color circles). The background raster displays snow depth estimated using airborne Light

https://doi.org/10.5194/egusphere-2026-986
Preprint. Discussion started: 16 June 2026

Detection and Ranging (LiDAR), while the black circles represent manual field measurements. The four marked sub-regions (1–5) highlight clustered areas for localized comparison (b) Spatial Distribution of Absolute Relative LiDAR Snow Depth Errors and Canopy Height at CPCRW.

4.2 Physical Influence on Error

We next analyzed how the LiDAR snow depth error (LiDAR minus ground measurements) varies with the environmental factors of interest (canopy height, slope, surface roughness, elevation and ground point density). Figure 7 shows that higher canopy classes tend to have a larger proportion of high-error cases. In low-canopy areas (0–5 m), high errors (Absolute relative error ≥ 0.5, 50%) account for only about 3% of the points, with most observations in the low-error range (Absolute relative error ≤ 0.25, 25%). In contrast, canopy heights of 10–15 m, 15–20 m, and ≥ 20 m exhibit markedly higher proportions of high-error cases (up to 14–15%), along with a noticeable reduction in the proportion of low-error cases.

A logistic regression using canopy height as a continuous predictor confirmed this trend: each 1 m increase in canopy height was associated with a 9.1% increase in the odds of a high error (Absolute relative error ≥ 0.5, 50%) (odds ratio = 1.091, $p < 0.00001$). Using canopy height bins, the odds of high error in the 10–15 m, 15–20 m, and ≥ 20 m categories were approximately 4–6 times higher than in the 0–5 m reference group ($p < 0.01$ for all) (Figure 8).

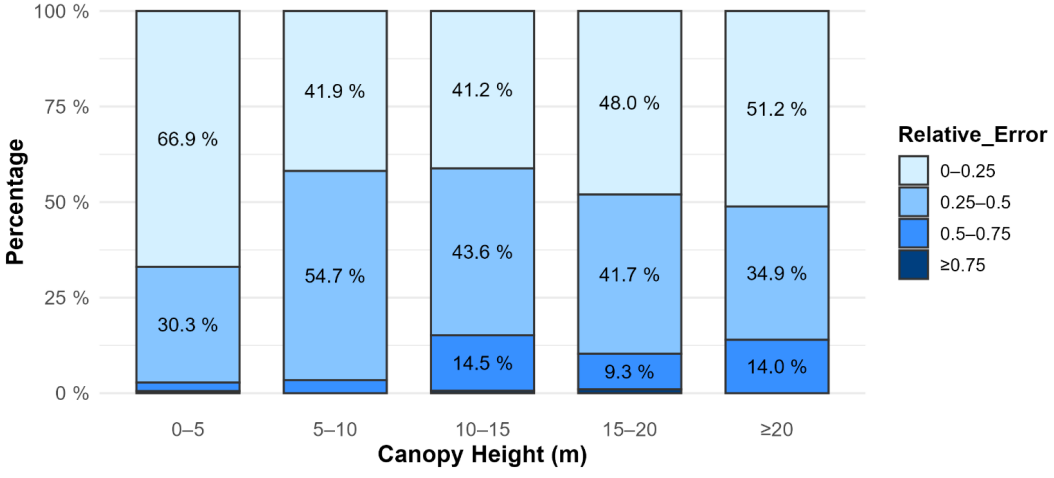

Figure 7. Distribution of LiDAR Snow Depth Relative Errors Across Canopy Height Categories

https://doi.org/10.5194/egusphere-2026-986
Preprint. Discussion started: 16 June 2026

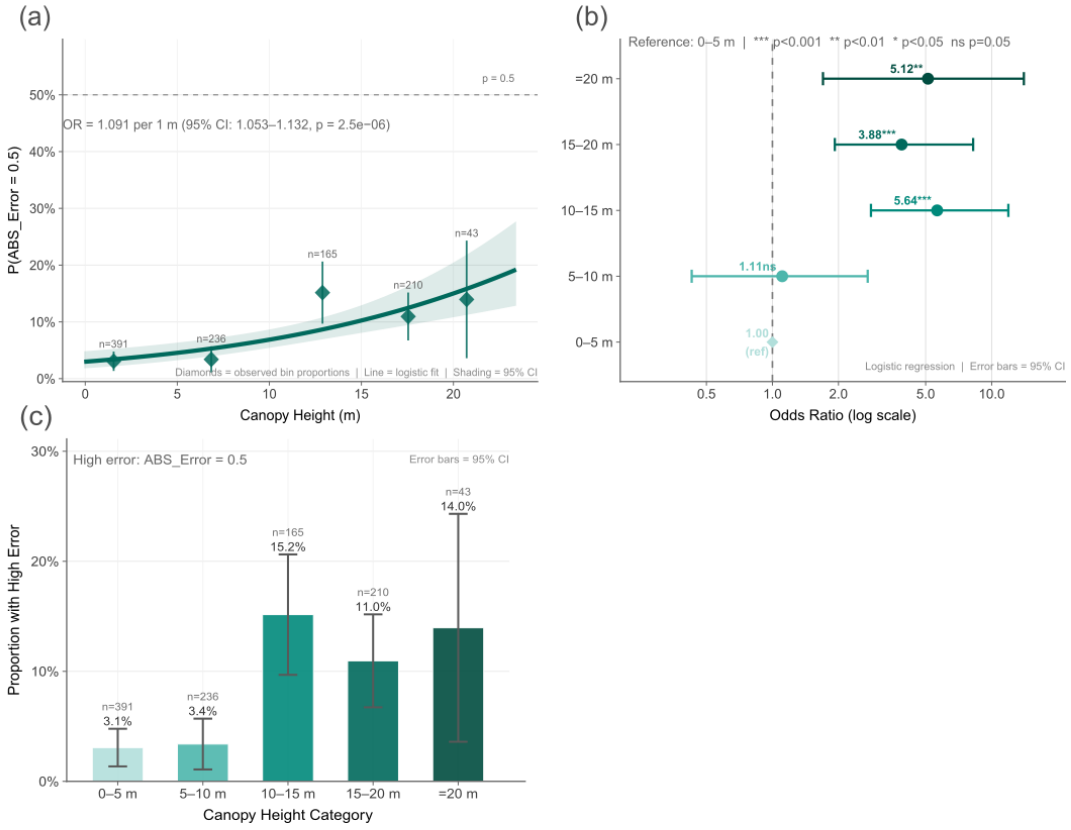

Figure 8. Relationship between canopy height and high LiDAR snow depth error (ABS_Error ≥ 0.5). (a) Logistic regression showing increasing probability of high error with canopy height. OR = 1.091 per 1 m increase (9.1% higher odds) (b) Odds ratios of high-error occurrence by canopy height category relative to the 0–5 m reference group. (c) Observed proportion of high-error cases across canopy height bins. Error bars indicate 95% confidence intervals.

Terrain slope was also an important factor affecting LiDAR snow-depth errors. Error magnitudes generally increased on steeper terrain. For example, the median absolute relative error was about 21% on gentle slopes (<5°) in CPCRW but increased to approximately 32% on slopes of 15–25° in FLCF. This pattern suggests that LiDAR measurements become more challenging in steep terrain (Figure 9a).

Surface roughness showed a moderate influence on LiDAR snow-depth error. Error magnitudes were generally similar across most roughness classes, although locations with very high roughness (>0.15 m) exhibited substantially larger errors in FLCF, where the median absolute relative error reached approximately 50%. Overall, the relationship between roughness and error was less consistent than that observed for canopy height, suggesting that roughness is a secondary factor influencing LiDAR performance (Figure 9b).

https://doi.org/10.5194/egusphere-2026-986
Preprint. Discussion started: 16 June 2026

As a standalone factor, no consistent monotonic relationship between elevation and error was observed within individual sites. Although CPCRW exhibited both higher elevations and larger errors, this likely reflects site-specific conditions rather than a direct elevation effect. Within each site, elevation differences did not noticeably impact LiDAR performance after accounting for local slope and canopy. Therefore, elevation is acting as a proxy for site characteristics rather than a direct influence on error.

Ground point density showed a moderate relationship with LiDAR snow-depth error. Locations with lower ground point density generally exhibited larger errors, particularly in CPCRW and FLCF. In contrast, higher-density areas tended to have smaller errors, suggesting that sufficient ground returns improve terrain characterization beneath the snowpack. Many low-density observations occurred beneath taller canopies, indicating that canopy occlusion may reduce the number of laser pulses reaching the ground surface (Figure 9c).

Ground point density tends to decrease with increasing canopy height, reflecting the structural limitation of laser penetration under taller canopies rather than a strong linear relationship (see Figure S1 in the Supplementary Information). Ground point density showed a weak but significant negative relationship with canopy height in all three regions. The strongest relationship was observed in CPCRW ($R^2 = 0.10$, $p < 0.001$), indicating that taller canopies generally produced fewer ground returns.

To illustrate these relationships, Figure 10 presents the relative importance of each factor as determined by the GBM model.

Canopy height was consistently the top predictor across all models. In all three site GBM model, canopy height was the most important variable. Especially in FLCF, canopy height alone accounted for about 35% of the total model decision splits (relative importance ~35%), whereas the second-ranked variable (slope) was around 24%, and the third-ranked variable (roughness) was around 22%, while others were each <15%. In other site models, the dominance of canopy remained: for BCEF and CPCRW, canopy was ~28% of importance in GBM.

In addition to the environmental predictors examined above, we further investigated the influence of vegetation type on LiDAR snow depth errors. Across the entire SnowEx 2023 domain, six vegetation classes are defined; however, the study sites analyzed here are limited to evergreen forest and deciduous forest. Our analysis indicates that, while snow depth values are generally higher in evergreen forests than in deciduous forests, the relative error distributions between the two vegetation types are remarkably similar. This suggests that although vegetation type influences the spatial distribution of snow depth, its impact on LiDAR-derived snow depth errors is comparatively limited. These results are illustrated in Figs. S2 and S3. In addition, we extended this analysis to all available SnowEx 2023 datasets, including the other two study regions (i.e., ACP and UKT), as shown in Figs. S4 and S5.

https://doi.org/10.5194/egusphere-2026-986
Preprint. Discussion started: 16 June 2026

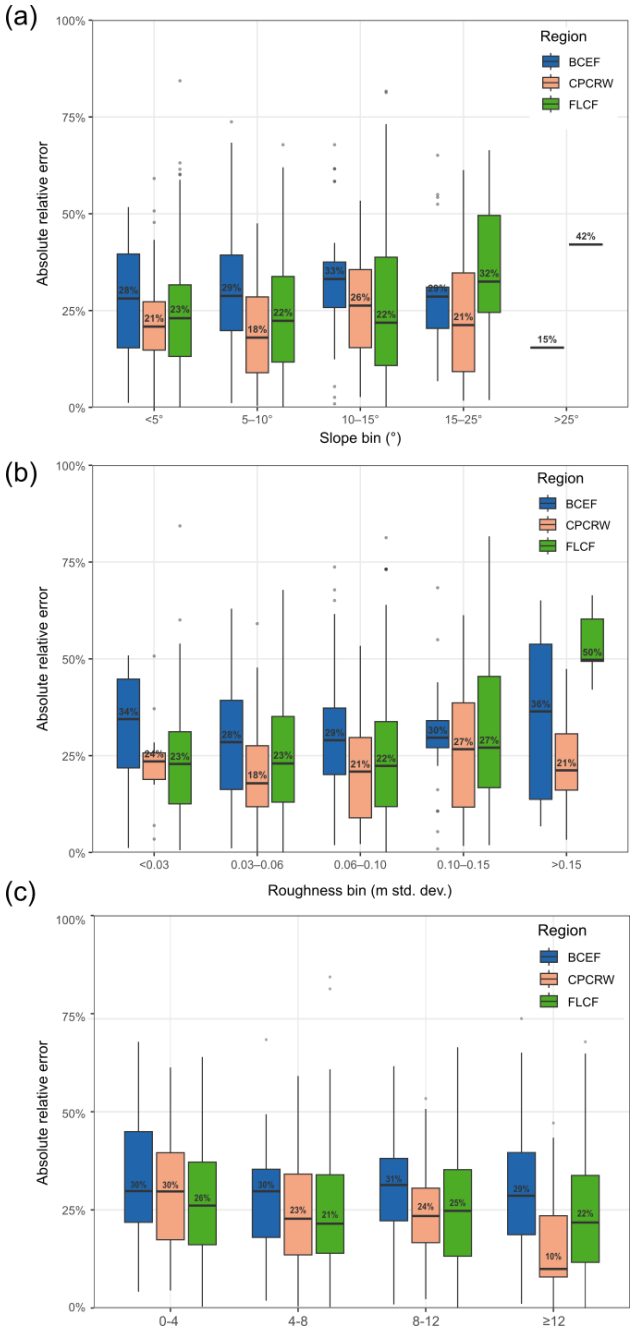

Figure 9. Influence of Environmental Factors on LiDAR Snow Depth Errors Across BCEF, CPCRW, and FLCF. (a) Absolute relative LiDAR snow depth errors across terrain slope classes in BCEF, CPCRW, and FLCF. (b) Absolute relative LiDAR snow depth errors across surface roughness classes in BCEF, CPCRW, and FLCF. (c) Absolute relative LiDAR snow depth errors across ground point density classes in BCEF, CPCRW, and FLCF.

https://doi.org/10.5194/egusphere-2026-986
Preprint. Discussion started: 16 June 2026

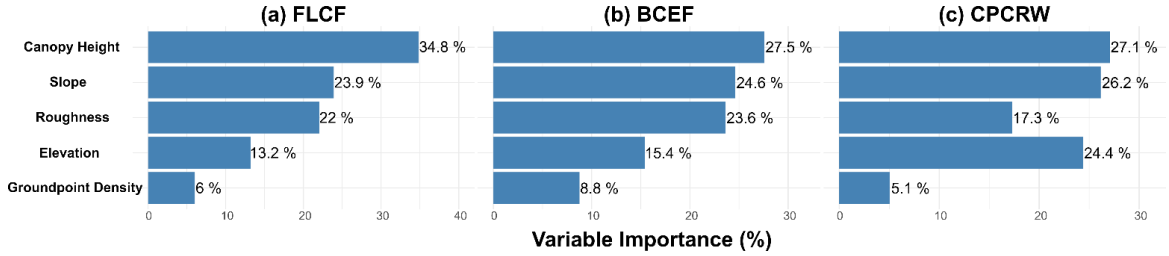

Figure 10. Relative importance of environmental variables in predicting LiDAR snow depth error (from the GBM model). Canopy height is by far the most influential factor, followed by slope. Roughness and elevation have smaller contributions, and ground point density is least influential once canopy is accounted for.

As shown in Figure 10, the influence of slope was consistently important across all three sites, ranking as the second most contributing factor. In CPCRW's model, slope importance (26.2%) was nearly equal to canopy height (27.1%). Even in FLCF (largely flat), slope still exhibited substantial importance (23.9%). Elevation showed varying importance; it was secondary in FLCF and BCEF, but emerged as a major factor in CPCRW (24.4%), nearly matching slope and canopy height. Ground point density remained the least important predictor across all individual site models.

In summary, the exploratory analysis and variable importance both point to forest canopy height (density) as the primary driver of LiDAR snow depth error, with terrain slope as a notable secondary factor. These factors explain why errors were largest in densely treed, steep areas (like parts of CPCRW) and smallest in open, flat areas (like parts of FLCF). The findings are consistent with qualitative expectations: dense vegetation prevents LiDAR from seeing the snow, and steep slopes complicate the geometry of LiDAR measurement.

4.3 Model Performance and Error Prediction

To quantify the control drivers of snow depth errors, we used a GBM model to predict spatial errors and identify the contributing input variables. Given the inherent variability and some unmodeled factors (and possible measurement noise), this is a reasonable performance, it indicates the models captured nearly half of the variation in LiDAR error using just these five predictors.

Looking at specific site models: the CPCRW GBM model was the best, with $R^2 = 0.527$ (about 53% of error variance explained). This higher performance at CPCRW may be because CPCRW had the widest range of terrain and slope conditions, giving the model more signal to latch onto. The BCEF model had R^2 ~0.33, and FLCF was lower, ~0.18. The models confirm quantitatively the influence of each factor. For example, in the CPCRW GBM model, canopy height showed the strongest influence on predicted LiDAR snow depth error (Figure 11d). Relative error decreased from approximately -0.20 at low canopy heights to about -0.30 at canopy heights above 7–8 m, indicating increased underestimation under taller canopies. Slope exhibited a weaker non-linear effect, with relative error decreasing from about -0.13 at low slopes to approximately -0.19 at moderate slopes before stabilizing (Figure 11a). Roughness was associated with progressively more negative errors, particularly above 0.12–0.15 m (Figure 11b). Ground point density showed a threshold-like response

https://doi.org/10.5194/egusphere-2026-986
Preprint. Discussion started: 16 June 2026

(Figure 11c): relative error became less negative when density exceeded approximately 10 pts m^{-2} and remained relatively stable thereafter.

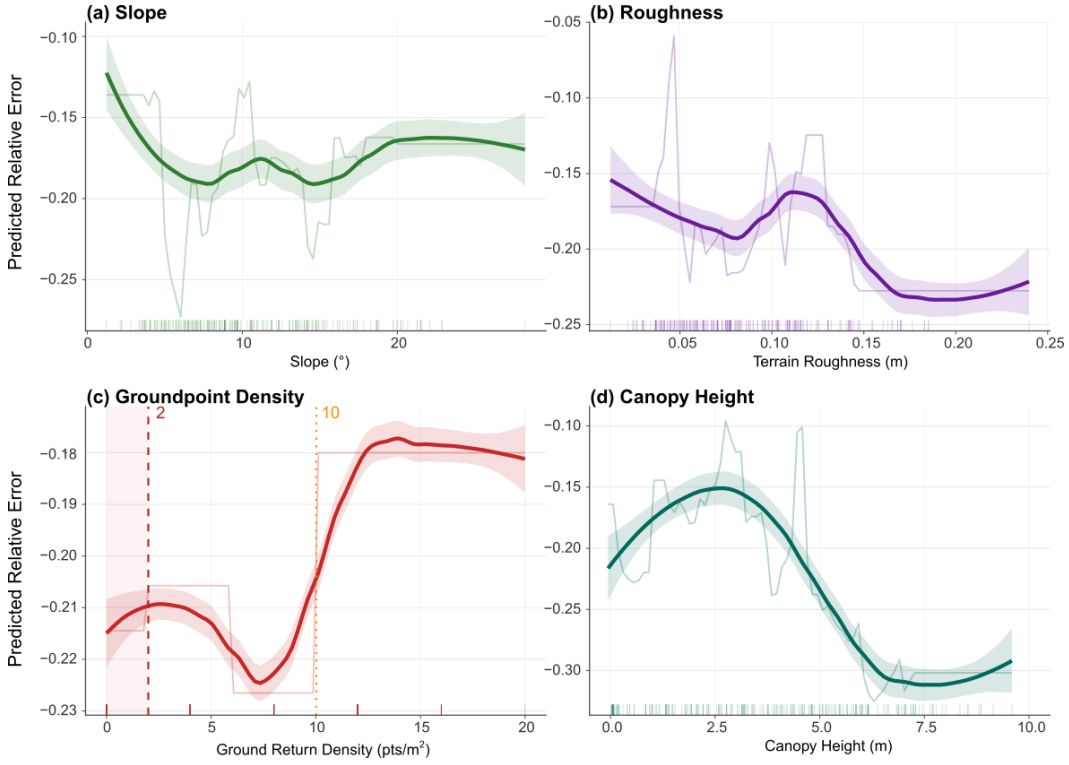

Figure 11. Partial dependence plots illustrating the influence of terrain slope, surface roughness, ground return density, and canopy height on LiDAR snow depth relative error. Shaded bands represent 95% confidence intervals, and rug marks indicate the distribution of observations.

To visualize model outcomes spatially, we applied the BCEF GBM model across the BCEF subregion as a gridded prediction of error. Figure 12 shows the resulting map of predicted LiDAR snow depth errors over the BCEF region. In Figure 12, Blue tones (underestimation) clearly correspond to known dense spruce of BCEF. Red areas (overestimation) are scarce, but a few open areas show LiDAR might slightly over-predict. The spatial patterns from the model closely match what we observed in the actual data points and provide confidence that the model is capturing real effects: essentially, it "flags" the same trouble spots the ground truth did at dense forests and steep, complex terrain.

In summary, the modeling results reinforce that canopy height is the dominant control on LiDAR snow depth error across these boreal forest sites, with slope as a second contributor. The predictive models can reasonably estimate error given those factors (R^2 up to 0.53), which is useful for identifying where LiDAR measurements are likely reliable or not. This approach of error prediction could be applied to correct or filter LiDAR-derived

https://doi.org/10.5194/egusphere-2026-986
Preprint. Discussion started: 16 June 2026

snow products by accounting for these variables.

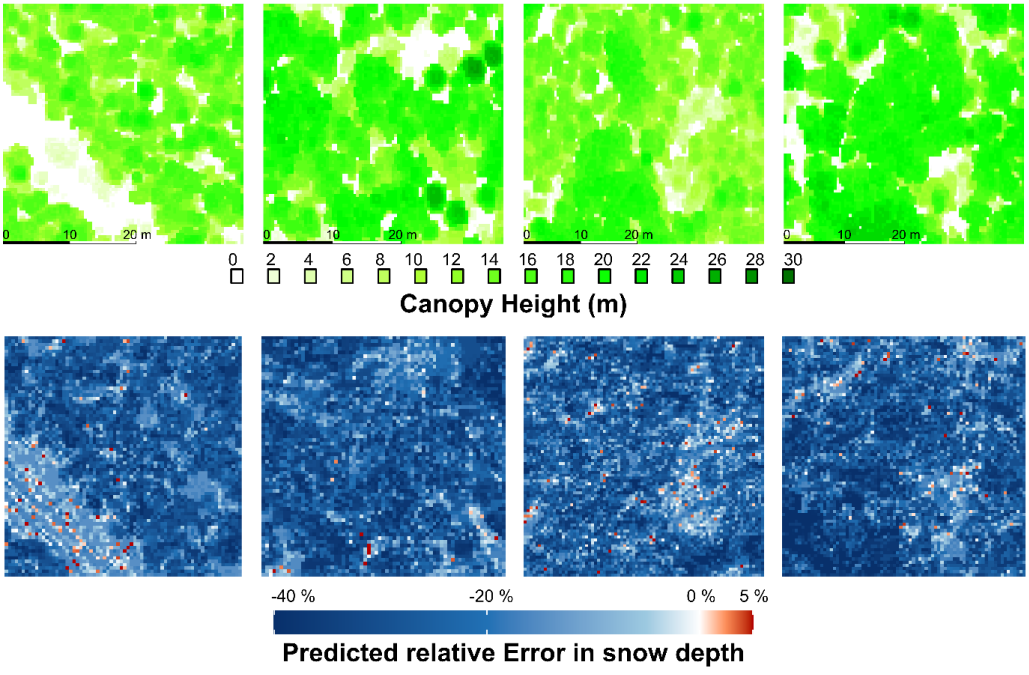

Figure 12. Canopy height (top row) and GBM-predicted relative LiDAR snow depth error (bottom row) across representative BCEF subregions. GBM-predicted spatial distribution of LiDAR snow depth error across part of the BCEF site. Warmer colors (red) indicate areas where LiDAR is predicted to overestimate snow depth (positive error), while cooler colors (blue) would indicate underestimate (negative error). The model predicts higher errors in densely forested areas and on steep slopes, whereas lower errors are expected in open areas. This spatial prediction aligns with the field observations that LiDAR struggled under the darkest forest canopy.

5. Discussion

5.1 Airborne LiDAR performance in boreal forest environments

Our evaluation of airborne LiDAR for snow depth mapping in boreal forests indicates a moderate level of performance. An overall MAD of 19 cm and correlation 0.6 suggests that airborne LiDAR, even with a high-quality sensor and survey design, does experience notable accuracy degradation under forest canopies. In open environments, previous studies have found airborne LiDAR can achieve errors on the order of just a few centimeters. For instance, Jacobs et al. (2021) used a UAS LiDAR in a mixed forest/open area and reported ~1 cm error in open field conditions, but ~10 cm error under forest canopy. Our findings are consistent with that gap: the forested areas in our study similarly show an order of magnitude larger error than open areas. However, unlike the Jacobs et al. study which dealt with an exceptionally shallow snowpack (<20 cm), we looked at a deeper snow regime (~50 cm typical) and still see around 20–30% relative errors in forests. These findings confirm that the influence of canopy structure on LiDAR accuracy remains significant across varying

https://doi.org/10.5194/egusphere-2026-986
Preprint. Discussion started: 16 June 2026

snow depths and forest conditions.

It's worth noting that our airborne LiDAR point density (10–20 pts/m²) is lower than that of UAS-based surveys (which can exceed 100 pts/m²). The lower point density, combined with the larger scan angle and higher altitude, likely contributes to reduced penetration in dense canopy. Yet, our results demonstrate that even at ~20 pts/m², enough ground returns were obtained to produce a meaningful snow depth map; the challenge is the quality and distribution of those returns under canopy. The moderate correlation of 0.6 across mixed conditions indicates that airborne LiDAR is capturing the general pattern of snow distribution (e.g., distinguishing which areas have more snow than others), but the scatter around the 1:1 line reveals uncertainty that matters for quantitative uses (like estimating water volume). In a hydrologic modeling context, a 0.19 m MAD might be acceptable for some purposes (e.g., broad water supply estimation), but for process studies or evaluating fine-scale snow dynamics, improvements are needed.

Encouragingly, not all forest areas suffered large errors – stands of shorter trees or more open canopy allowed LiDAR to perform well (often within 5–10 cm of in-situ). This implies that airborne LiDAR retains significant utility in patchy forest landscapes. Purely from an operational perspective, one might consider combining LiDAR with other data (e.g., canopy maps) to flag areas of likely underestimation. Our modeling in fact moves in that direction by predicting error from canopy characteristics.

5.2 Comparison with previous studies

Relatively few studies have directly quantified airborne LiDAR snow depth accuracy in dense forests (Currier et al., 2019), but our results align with the trends reported in related work. Besides Jacobs et al. (2021) mentioned above, Deems et al. (2013) noted in their review that forested areas are prone to higher errors and highlighted the importance of scan angle and pulse density in such terrain. They pointed out that near-infrared LiDAR pulses can be scattered within the snowpack and by vegetation, complicating returns. Our findings of underestimation under canopy are consistent with the notion that some laser energy is either not reaching the ground or is returning from slightly below the true snow surface (due to scattering within the snow or hitting lower branches).

A study by Helfricht et al. (2014) in alpine terrain (not forest, but deep snow on glaciers) found that airborne LiDAR tend to underestimate snow depth in high-accumulation areas by on average ~0.4 m when compared to ground-penetrating radar. They attributed this partly to the inability of LiDAR to capture very soft, low-density snow at the surface and possible penetration into the snow. While their environment is different (open glacier), the underestimation pattern is similar to what we see under trees – in both cases, LiDAR reports less snow than ground truth in certain conditions. This suggests a common thread: whether due to volumetric penetration (in soft snow) or occlusion (by vegetation), LiDAR returns may originate below the actual snow surface, yielding underestimates.

Our identification of canopy height as the top error driver is in line with general understanding of snow interception and LiDAR occlusion. Tall, dense canopies intercept snowfall (reducing actual snow on ground)

https://doi.org/10.5194/egusphere-2026-986
Preprint. Discussion started: 16 June 2026

and also block the LiDAR pulses. Thus, there is a compound effect: beneath a dense canopy, the snowpack is not only thinner to begin with (due to interception losses), but the LiDAR also has difficulty measuring whatever snow is there. Pomeroy and Gray (1995) and Schmidt and Gluns (1991) documented how coniferous canopies can retain a large fraction of snowfall, leading to much lower snow depths under trees; our forest measurement points indeed often had much less snow than nearby clearings, reflecting these processes. Jacobs et al. (2021) observed significantly shallower snow in conifer stands compared to open areas (even in their 10 cm total snowfall event). We add that LiDAR underestimation exacerbates the discrepancy in measured vs actual snow under canopy.

Terrain slope being a significant factor also echoes findings from previous topographic studies of snow distribution. While slope mainly influences snowpack through redistribution (steep slopes hold less snow and lose snow more easily), it also geometrically affects LiDAR accuracy. In photogrammetry, steep slopes cause larger errors due to viewing angle; similarly with LiDAR, the pulse footprint elongates on slopes and small GPS/INS errors translate to vertical errors on steep inclines. Our data showed ~5–15 cm worse errors on slopes >20°. Jacobs et al. also noted that areas with steep slopes had higher snow depth confidence intervals and somewhat reduced LiDAR performance. Thus, both our study and others highlight slope as a risk factor for remote sensing of snow.

Compared to the example study by Cho et al. (2021), which used a Maximum Entropy model to find drivers of snow depth heterogeneity in a mixed open/forest environment, there are parallels in the importance of vegetation and terrain. Cho et al. found that vegetation type (open vs forest) and terrain roughness were among the most important predictors of snow presence or depth patterns. In our case, those same factors (canopy, roughness) are critical but with respect to measurement error rather than natural distribution. This suggests an interesting point: where vegetation strongly controls actual snow accumulation, it also controls measurement accuracy – the two are linked. One difference is that Cho et al. emphasized soil properties as well (relevant for shallow snow). As airborne LiDAR does not directly observe conditions beneath the snowpack, subsurface soil properties were beyond the scope of this analysis.

Building on this line of research, May et al. (2025) further highlighted canopy effects in CPCRW, and our study extends their work to multiple boreal subregions with a machine learning framework. We found that canopy height consistently emerged as the dominant factor, followed by slope, while other variables played minor roles. This broader scope and multi-factor approach highlights both the ecological controls on snow distribution and the mechanisms underlying LiDAR errors, offering practical pathways for improving airborne snow surveys in forested terrain.

5.3 Limitations and implications

First, the ground truth dataset, while fairly extensive (1,045 points), is still relatively sparse over a large area. It is possible that our point measurements do not capture all micro-scale variability. For example, under a tall tree, snow depth can vary within a few meters due to drip zones, microtopography, or vegetation cover. A

https://doi.org/10.5194/egusphere-2026-986
Preprint. Discussion started: 16 June 2026

single probe might read 40 cm, but just a few meters away the depth could be 30 cm. The LiDAR, averaging over a 1 m grid cell, might legitimately pick up a different value than the probe, especially if the probe happened to hit a locally deeper or shallower spot. While our study attempted to mitigate this by sampling a large number of points, some amount of residual error arises from snow variability at scales below the LiDAR resolution. One effective strategy to reduce this limitation, as demonstrated in Cho et al. (2024), is to conduct multiple depth measurements within each 1 × 1 m grid cell—specifically, nine measurements per cell. This approach helps average out fine-scale heterogeneity and yields a more representative comparison between LiDAR-derived and ground-based measurements. Such sampling designs may be particularly beneficial in heterogeneous forested terrain where sub-meter variability is high.

Second, the design of the manual snow depth measurement tool (i.e., manual probe) may also introduce errors. The probe requires downward insertion into the snowpack to record depth. There is a risk that the probe tip penetrates slightly into the soil or underlying organic layer during measurement, especially when snow is soft or the operator applies excess force. This could result in a manual depth reading that is slightly larger than the actual snow depth, contributing to a small but systematic positive bias in ground-based measurements. Consequently, LiDAR-derived snow depths may appear negatively biased even when they accurately reflect the snow surface. (Proulx et al., 2023, Stuefer et al., 2025)

Third, the positional accuracy of the ground-based snow depth measurements may also degrade the comparison between in-situ and LiDAR data. As reported in May et al. (2025), the manual probe GPS has a horizontal positioning error of ±2.5 m in open areas and can increase up to 10–15 m in dense forest. Given the high spatial variability of snow depth at sub-meter scales—often observed to vary by several centimeters within 1 m due to microtopography, vegetation, or drip zones—this spatial mismatch can significantly obscure the correlation between collocated ground and LiDAR measurements.

Despite these limitations, the implications of our findings are quite relevant for practical snow remote sensing. Knowing that tall canopy is the Achilles heel of LiDAR snow measurement means that forest snow mapping efforts should consider complementary approaches in those areas. One approach could be to integrate satellite LiDAR or photogrammetry from different angles, or even incorporate ground-penetrating radar for under-canopy snow (as some SnowEx studies have tested). Our error prediction maps (like Fig. 4.6) could be used as an uncertainty layer, flagging areas of potential underestimation so that hydrologists or modelers can treat those with caution. For example, one could imagine using the predicted error to correct the LiDAR snow depths: if the model expects LiDAR under-shot by 30% under certain trees, one could adjust the depth accordingly (with large uncertainty bounds). Another implication is for the design of future LiDAR surveys. As mentioned, increasing point density in problem areas could improve results. This could be done by flying slower, lower, or with cross-track or multi-angle LiDAR if available. The cost is increased flight time, but if a particular forest basin is critical (say for water supply), it might be worth flying twice in different directions to fill in the gaps. Additionally, waveform LiDAR (recording the full return waveform) could potentially retrieve some information even when discrete returns fail. The Riegl sensor used does have waveform capability;

https://doi.org/10.5194/egusphere-2026-986
Preprint. Discussion started: 16 June 2026

analysis of waveform could be a next step to see if it indicates energy attenuation that correlates with snow.

6. Conclusions

We investigated the accuracy of airborne LiDAR for measuring snow depth in the boreal forests of interior Alaska and analyzed the environmental factors influencing any measurement errors. Using data from the NASA SnowEx 2023 campaign, we compared LiDAR-derived snow depths to extensive ground truth and found that LiDAR can capture snow depth patterns in forested terrain with moderate success: overall correlation ~0.60 and mean absolute error ~0.19 m. However, accuracy is not uniform – LiDAR performed best in open or lightly forested areas (often within ~20% of truth) and worst under dense canopies and on steep slopes (errors of ~30% or more, typically underestimating the snow). By applying machine learning models, we identified canopy height as the dominant driver of LiDAR snow depth errors, with taller vegetation leading to greater underestimation. Terrain slope was the second most important factor, also contributing to underestimation on steeper grades. Other factors like surface roughness and elevation played secondary roles, and low ground point density was associated with larger errors but largely because it occurs in areas of tall canopy. Our results underscore that while airborne LiDAR is a powerful tool for snow depth mapping over broad areas, users must be aware of its limitations in forested landscapes. In particular, depths retrieved beneath mature boreal forest can significantly under-represent true snow accumulation. The consistency of canopy influence across three distinct sites suggests that this is a general phenomenon in boreal forests and likely in other forest types as well. On the positive side, the errors are not random: they correlate with observable features (trees and slopes), meaning we can predict where LiDAR will have trouble. This opens the door to incorporating correction factors or uncertainty estimates into LiDAR-based snow products. For instance, one could imagine adjusting LiDAR depths upward in areas of very tall canopy to compensate for expected under-measurement, using relationships like those quantified here. In conclusion, airborne LiDAR remains an invaluable method for snow depth measurement, offering unparalleled high-resolution coverage, but for full reliability in forested regions it should be complemented by careful validation and error modeling. The SnowEx 2023 Alaska dataset, with its combination of remote sensing and ground observations, has allowed us to pinpoint the weaknesses of LiDAR under forest cover and to suggest ways to improve future estimates.

Data Availability

All data used in this study are publicly available. The airborne LiDAR and snow depth measurements were obtained from the NASA SnowEx 2023 Alaska Campaign and can be accessed through the NASA Earthdata portal: https://search.earthdata.nasa.gov. Additional field measurement data (e.g., in-situ snow depths) are available via the National Snow and Ice Data Center (NSIDC): https://nsidc.org/data/snex23_mar23_sd/versions/1. To reproduce the results, including figures, R scripts, and processed data, all materials are openly available on Zenodo [*link to be added from Zenodo, currently being*

https://doi.org/10.5194/egusphere-2026-986
Preprint. Discussion started: 16 June 2026

setup with an ODC Attribution (ODC-BY) license for access without restrictions].

Competing Interests

The contact author has declared that none of the authors has any competing interests.

Acknowledgements

I would like to sincerely thank the NASA SnowEx 2023 Science Team and all campaign participants for their dedication and support. Their collective efforts made the data collection possible and were essential to the success of this research. I am especially grateful to Svetlana Stuefer for leading the campaign and to Chris Larsen at the University of Alaska Fairbanks for piloting the aircraft throughout the field campaign. JP and EC were supported by the NASA Subseasonal-to-Seasonal Hydrometeorological Prediction Program (Grant No. 80NSSC24K1278), the Bureau of Reclamation Snow Water Supply Forecasting Program (Grant No. R24AC00021-00), and the Ingram School of Engineering at Texas State University.

References

[1] Xu, L., & Dirmeyer, P. (2013). Snow–Atmosphere Coupling Strength. Part II: Albedo Effect Versus Hydrological Effect. Journal of Hydrometeorology, 14(2), 404–418. https://doi.org/10.1175/JHM-D-11-0103.1

[2] Blau, M. T., Kad, P., Turton, J. V., & Ha, K. J. (2024). Uneven global retreat of persistent mountain snow cover alongside mountain warming from ERA5-land. *npj Climate and Atmospheric Science, 7*(1), 278. https://doi.org/10.1038/s41612-024-00829-5

[3] Stewart, I. T., Cayan, D. R., & Dettinger, M. D. (2004). Changes in Snowmelt Runoff Timing in Western North America under a 'Business as Usual' Climate Change Scenario. *Climatic Change, 62*(1-3), 217–232. https://doi.org/10.1023/B:CLIM.0000013702.22656.e8

[4] Fritze, H., Stewart, I. T., & Pebesma, E. (2011). Shifts in Western North American Snowmelt Runoff Regimes for the Recent Warm Decades. *Journal of Hydrometeorology, 12*(5), 989–1006. https://doi.org/10.1175/2011JHM1360.1

[5] Lundquist, J. D., & Dettinger, M. D. (2005). How snowpack heterogeneity affects diurnal streamflow timing. *Water Resources Research, 41*(5). https://doi.org/10.1029/2004WR003649

[6] Varhola, A., Coops, N. C., Weiler, M., & Moore, R. D. (2010). Forest canopy effects on snow accumulation and ablation: An integrative review of empirical results. *Journal of Hydrology, 392*(3-4), 219–233. https://doi.org/10.1016/j.jhydrol.2010.08.009

[7] Guan, X., Zeng, X., Shi, R., Chen, H., & Wei, Z. (2023). Changes in snow parameterization over typical vegetation in the Northern Hemisphere. *Atmospheric and Oceanic Science Letters, 16*(2), 100325. https://doi.org/10.1016/j.aosl.2022.100325

[8] Stillinger, T., Rittger, K., Raleigh, M. S., Michell, A., Davis, R. E., & Bair, E. H. (2023). Landsat, MODIS,

https://doi.org/10.5194/egusphere-2026-986
Preprint. Discussion started: 16 June 2026

and VIIRS snow cover mapping algorithm performance as validated by airborne lidar datasets. *The Cryosphere, 17*(2), 567–590. https://doi.org/10.5194/tc-17-567-2023

[9] Luo, J., Dong, C., Lin, K., Chen, X., Zhao, L., & Menzel, L. (2022). Mapping snow cover in forests using optical remote sensing, machine learning and time-lapse photography. *Remote Sensing of Environment, 275*, 113017. https://doi.org/10.1016/j.rse.2022.113017

[10] Rittger, K., Raleigh, M. S., Dozier, J., Hill, A. F., Lutz, J. A., & Painter, T. H. (2020). Canopy Adjustment and Improved Cloud Detection for Remotely Sensed Snow Cover Mapping. *Water Resources Research, 56*(6). https://doi.org/10.1029/2019WR024914

[11] Demil, G., Haghighi, A. T., Klöve, B., & Oussalah, M. (2025). Advances in image-based estimation of snow variable: A systematic literature review on recent studies. *Journal of Hydrology, 654*, 132855. https://doi.org/10.1016/j.jhydrol.2025.132855

[12] Lumbrazo, C., Bennett, A., Currier, W. R., Nijssen, B., & Lundquist, J. (2022). Evaluating Multiple Canopy-Snow Unloading Parameterizations in SUMMA With Time-Lapse Photography Characterized by Citizen Scientists. *Water Resources Research, 58*(6). https://doi.org/10.1029/2021WR030852

[13] Dharmadasa, V., Kinnard, C., & Baraër, M. (2024). Meteorological control on snow depth evolution and snowpack energy exchanges in an agro-forested environment by a measurement-based approach. *Agricultural and Forest Meteorology, 347*, 109915. https://doi.org/10.1016/j.agrformet.2024.109915

[14] Deems, J. S., Painter, T. H., & Finnegan, D. C. (2013). Lidar measurement of snow depth: a review. *Journal of Glaciology, 59*(215), 467–479. https://doi.org/10.3189/2013JoG12J154

[15] Clark, M. L., & Clark, D. B. (2004). Small-footprint lidar estimation of sub-canopy elevation and tree height in a tropical rainforest landscape. *Remote Sensing of Environment, 91*(1), 68–89. https://doi.org/10.1016/j.rse.2004.02.008

[16] Jacobs, J. M., Hunsaker, A. G., Sullivan, F. B., Palace, M., Burakowski, E. A., Herrick, C., & Cho, E. (2021). Snow depth mapping with unpiloted aerial system lidar observations: A case study in Durham, New Hampshire, United States. *The Cryosphere, 15*(3), 1485–1500. https://doi.org/10.5194/tc-15-1485-2021

[17] Dharmadasa, V., Kinnard, C., & Baraër, M. (2022). An Accuracy Assessment of Snow Depth Measurements in Agro-Forested Environments by UAV Lidar. *Remote Sensing, 14*(7), 1649. https://doi.org/10.3390/rs14071649

[18] May, L. D., Stuefer, S. L., Goddard, S. D., & Larsen, C. F. (2025). Analyzing vegetation effects on snow depth variability in Alaska's boreal forests with airborne lidar. *The Cryosphere, 19*(9), 3477–3492. https://doi.org/10.5194/tc-19-3477-2025

[19] Hojatimalekshah, A., Gongora, J., Enterkine, J., Glenn, N. F., Caughlin, T. T., Marshall, H. P., & Hiemstra, C. A. (2023). Lidar and deep learning reveal forest structural controls on snowpack. *Frontiers in Ecology and the Environment, 21*(1), 49–54. https://doi.org/10.1002/fee.2584

[20] Hojatimalekshah, A., Uhlmann, Z., Glenn, N. F., Hiemstra, C. A., Tennant, C. J., Graham, J. D., et al.

https://doi.org/10.5194/egusphere-2026-986
Preprint. Discussion started: 16 June 2026

(2021). Tree canopy and snow depth relationships at fine scales with terrestrial laser scanning. *The Cryosphere, 15*(5), 2187–2209. https://doi.org/10.5194/tc-15-2187-2021

[21] Meriö, L.-J., Rauhala, A., Ala-aho, P., Kuzmin, A., Korpelainen, P., Kumpula, T., Kløve, B., & Marttila, H. (2023). Measuring the spatiotemporal variability in snow depth in subarctic environments using UASs – Part 2: Snow processes and snow–canopy interactions. *The Cryosphere, 17*(10), 4363–4380. https://doi.org/10.5194/tc-17-4363-2023

[22] Gustafson, J. R., Brooks, P. D., Molotch, N. P., & Veatch, W. C. (2010). Estimating snow sublimation using natural chemical and isotopic tracers across a gradient of solar radiation. *Water Resources Research, 46*(12). https://doi.org/10.1029/2009WR009060

[23] Dadic, R., Mott, R., Lehning, M., & Burlando, P. (2010). Wind influence on snow depth distribution and accumulation over glaciers. *Journal of Geophysical Research: Earth Surface, 115*(F1). https://doi.org/10.1029/2009JF001261

[24] NASA. (2025). Cessna T206 used to fly lidar and optical sensors over SnowEx study sites. Retrieved from https://snow.nasa.gov/campaigns/snowex-2023-tundra-and-boreal-forest

[25] Li, D., Wrzesien, M. L., Durand, M., Adam, J., & Lettenmaier, D. P. (2017). How much runoff originates as snow in the western United States, and how will that change in the future? Geophysical Research Letters, 44(12), 6163–6172. https://doi.org/10.1002/2017GL073551

[26] Siirila-Woodburn, E. R., Rhoades, A. M., Hatchett, B. J., Huning, L. S., Szinai, J., Tague, C., ... & Kaatz, L. (2021). A low-to-no snow future and its impacts on water resources in the western United States. Nature Reviews Earth & Environment, 2(11), 800–819. https://doi.org/10.1038/s43017-021-00219-y

[27] Sturm, M., Goldstein, M. A., & Parr, C. (2017). Water and life from snow: A trillion dollar science question. Water Resources Research, 53(5), 3534–3544. https://doi.org/10.1002/2017WR020840

[28] Painter, T. H., Berisford, D. F., Boardman, J. W., Bormann, K. J., Deems, J. S., Gehrke, F., ... & Winstral, A. (2016). The Airborne Snow Observatory: Fusion of scanning lidar, imaging spectrometer, and physically-based modeling for mapping snow water equivalent and snow albedo. Remote Sensing of Environment, 184, 139–152. https://doi.org/10.1016/j.rse.2016.06.018

[29] Mazzotti, G., Currier, W. R., Deems, J. S., Pflug, J. M., Lundquist, J. D., & Jonas, T. (2019). Revisiting snow cover variability and canopy structure within forest stands: Insights from airborne lidar data. Water Resources Research, 55(7), 6198–6216. https://doi.org/10.1029/2019WR024898

[30] Deschamps-Berger, C., Gascoin, S., Berthier, E., Deems, J., Gutmann, E., Dehecq, A., ... & Dumont, M. (2020). Snow depth mapping from stereo satellite imagery in mountainous terrain: Evaluation using airborne lidar data. The Cryosphere Discussions, 2020, 1–28. https://doi.org/10.5194/tc-2020-127

[31] Currier, W. R., Pflug, J., Mazzotti, G., Jonas, T., Deems, J. S., Bormann, K. J., ... & Lundquist, J. D. (2019). Comparing aerial lidar observations with terrestrial lidar and snow-probe transects from NASA's 2017 SnowEx campaign. Water Resources Research, 55(7), 6285–6294. https://doi.org/10.1029/2019WR024907

https://doi.org/10.5194/egusphere-2026-986
Preprint. Discussion started: 16 June 2026

[32] NASA. (2018). SnowEx Science Plan (Version 1.6). National Aeronautics and Space Administration. https://snow.nasa.gov/campaigns/snowex

[33] Cho, E., Verfaillie, M., Jacobs, J. M., Hunsaker, A. G., Sullivan, F. B., Palace, M., & Wagner, C. (2024). Characterizing spatial structures of field-scale snowpack using unpiloted aerial system (UAS) lidar and SfM photogrammetry. EGUsphere, 2024, 1–25. https://egusphere.copernicus.org/preprints/2024/egusphere-2024-1530/egusphere-2024-1530.pdf

[34] Proulx, H., Jacobs, J. M., Burakowski, E. A., Cho, E., Hunsaker, A. G., Sullivan, F. B., ... & Wagner, C. (2023). Brief communication: Comparison of in situ ephemeral snow depth measurements over a mixed-use temperate forest landscape. The Cryosphere, 17(8), 3435–3442. https://doi.org/10.5194/tc-17-3435-2023

[35] Stuefer, S. L., Hale, K., May, L. D., Mason, M., Vuyovich, C., Marshall, H. P., Vas, D., & Elder, K. (2025). Snow depth measurements from Arctic tundra and boreal forest collected during NASA SnowEx Alaska campaign. Scientific Data, 12, Article 919. https://doi.org/10.1038/s41597-025-03282-3

[36] Friedman, J. H. (2001). Greedy function approximation: A gradient boosting machine. Annals of Statistics, 29(5), 1189–1232. https://doi.org/10.1214/aos/1013203451

[37] Elith, J., Leathwick, J. R., & Hastie, T. (2008). A working guide to boosted regression trees. Journal of Animal Ecology, 77(4), 802–813. https://doi.org/10.1111/j.1365-2656.2008.01390.x

[38] Zhao, F., Guan, K., Bernacchi, C. J., Peng, B., Pan, M., Jiang, C., & Yang, Y. (2021). Detecting climate adaptation in agricultural production using interpretable machine learning methods. Scientific Reports, 11, 3165. https://doi.org/10.1038/s41598-021-82705-6

[39] Lary, D. J., Alavi, A. H., Gandomi, A. H., & Walker, A. L. (2016). Machine learning in geosciences and remote sensing. Geoscience Frontiers, 7(1), 3–10. https://doi.org/10.1016/j.gsf.2015.07.003

[40] Pelletier, C., Webb, G. I., & Petitjean, F. (2019). Temporal convolutional neural network for the classification of satellite image time series. Remote Sensing, 11(5), 523. https://doi.org/10.3390/rs11050523

[41] Sturm, M., Taras, B., Liston, G. E., Derksen, C., Jonas, T., & Lea, J. (2015). White water: Fifty years of snow research in *Water Resources Research* and the outlook for the future. *Water Resources Research, 51*(7), 4945–4965. https://doi.org/10.1002/2015WR017284

[42] Vuyovich, C., Stuefer, S., Durand, M., Marshall, H. P., Osmanoglu, B., Elder, K., Vas, D., Gelvin, A., Larsen, C., Pedersen, S., Hodkinson, D., Deeb, E., Mason, M., & Youcha, E. (2024). NASA SnowEx 2023 Experiment Plan (Draft). NASA Goddard Space Flight Center.

[43] Larsen, C. (2024). *SnowEx23 Airborne Lidar Scans Raw*. (SNEX23_Lidar_Raw, Version 1). [Data Set]. Boulder, Colorado USA. NASA National Snow and Ice Data Center Distributed Active Archive Center. https://doi.org/10.5067/LCWGONIUOEER. Date Accessed 11-13-2025.

[44] Larsen, C. (2024). *SnowEx23 Airborne Lidar-Derived 0.5M Snow Depth and Canopy Height*. (SNEX23_Lidar, Version 1). [Data Set]. Boulder, Colorado USA. NASA National Snow and Ice Data Center Distributed Active Archive Center. https://doi.org/10.5067/BV4D8RRU1H7U. Date Accessed 11-

https://doi.org/10.5194/egusphere-2026-986
Preprint. Discussion started: 16 June 2026

762 13-2025.
763 [45] Currier, W. R., Pflug, J., Mazzotti, G., Jonas, T., Deems, J. S., Bormann, K. J. et al. (2019). Comparing
764 aerial lidar observations with terrestrial lidar and snow-probe transects from NASA's 2017 SnowEx
765 campaign. *Water Resources Research*, *55*(7), 6285-6294.
766